An investigation of the low-temperature Faraday rotation spectrum of $BaFe_{12}O_{19}$

1997 J. Phys.: Condens. Matter 9 4761

(http://iopscience.iop.org/0953-8984/9/22/026)

J. Phys.: Condens. Matter **9** (1997) 4761–4768. Printed in the UK PII: S0953-8984(97)80063-X

An investigation of the low-temperature Faraday rotation spectrum of $BaFe_{12}O_{19}$

H J Masterson†, J G Lunney and J M D Coey

Department of Pure and Applied Physics, Trinity College, Dublin 2, Ireland

Received 4 December 1996

Abstract. The Faraday rotation spectra between 1.5 eV and 2.4 eV are examined for thin films of the hexagonal ferrite $BaFe_{12}O_{19}$, prepared by pulsed laser deposition. Fine spectral detail is observed at 24 K between 1.69 eV and 1.85 eV. A sharp paramagnetic transition at 1.69 eV, with an oscillator strength of 5×10^{-2}, is assigned to the $^6A_{1g}(^6S) \rightarrow {}^4T_{2g}(^4G)$ crystal field transition originating on the $4f_2$ octahedrally coordinated Fe^{3+} site. Somewhat weaker diamagnetic transitions above 1.73 eV are tentatively assigned to first-excited-state transitions in the 2b trigonal bipyramidal Fe^{3+} site. A broader feature with an extremum at 2.23 eV is considered to originate from the $^6A_1(^6S) \rightarrow {}^4T_2(^4G)$ transition in $4f_1$ tetrahedral sites.

1. Introduction

Hexagonal barium ferrite ($BaFe_{12}O_{19}$) is commonly known as a permanant magnet. It has potential in the magnetic recording industry as a high-information-density thin-film recording medium due to its high uniaxial anisotropy constant which can favour an orientation of the magnetic moment out of the plane of the film [1]. It is not surprising then that a considerable amount of research has been undertaken in view of the magnetic and magnetooptic recording potential of this particular material [2–4], or of Co- and Ti-doped $BaFe_{12}O_{19}$ [5–7]. However, quite apart from this, the $BaFe_{12}O_{19}$ compound is highly interesting as regards its fundamental optical and magnetooptical properties, due to its complex crystallographic and magnetic structure, and a complete understanding in the above regard poses quite a challenge. Figure 1 shows a (110) cross section of the $BaFe_{12}O_{19}$ crystal structure, while the reader is referred to reference [1] for a more detailed treatment. The iron cations are all ferric, and are are located in octahedral 12k, $4f_2$ and 2a sites, and tetrahedral $4f_1$ sites, in addition to a trigonal bipyramidal 2b site which is understood to be mainly responsible for the *c*-axis magnetic anisotropy [8], but which has not been well characterized optically. In fact, although optical and magnetooptical spectra of $BaFe_{12}O_{19}$ have been examined previously in the spectral region extending from the visible to the near infra-red [5, 6, 9, 10], no attempt has been made, to our knowledge, to examine the low-temperature spectral detail in terms of possible assignments of crystal-field transitions to the above optical centres. This paper attempts to rectify this situation by presenting, for the first time, the low-temperature Faraday rotation spectra of $BaFe_{12}O_{19}$ between 1.5 eV and 2.4 eV, and suggesting assignments of the spectral detail to crystal-field transitions originating from the various Fe^{3+} sites.

† Present address: National Microelectronics Research Centre, Cork, Ireland.

0953-8984/97/224761+08$19.50

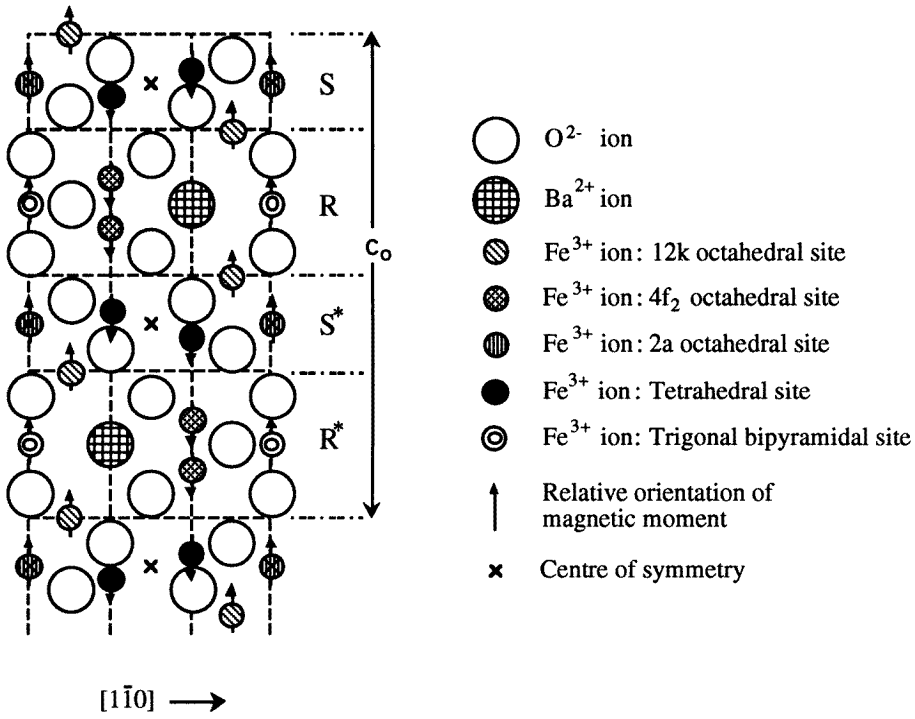

Figure 1. A (110) cross section of the crystal structure of $BaFe_{12}O_{19}$ constructed of S and R blocks and showing the various Fe^{3+} sites (S* and R* indicate a 180° rotational symmetry about the *c*-axis).

2. Experimental procedure

The samples of $BaFe_{12}O_{19}$ used for the present work were thin films, 1 μm thick, grown on (0001) sapphire substrates by pulsed laser deposition from a target of the same material. Details of this deposition technique can be found in a previous publication [11]. The samples were examined by x-ray diffraction after deposition, and were found to be of the correct phase, and oriented with the *c*-axis (the magnetic easy axis) out of the plane of the film. Scanning electron micrographs revealed films composed of hexagonal polycrystallites about 0.25 μm across.

Dispersive Faraday rotation spectra were recorded using the apparatus shown in figure 2. The apparatus consists of an S1000 diode array fibre-optic spectrometer from Ocean Optics Incorporated, a closed-cycle helium refrigerator situated between the pole pieces of an electromagnet and containing the sample, and a visible-light source. Optic fibres, carrying light to and from the sample, are connected to vacuum-coupled collimators on the walls of the fridge, behind which a polarizer and analyser are situated respectively on the input and output sides. These are oriented at 45° to each other with the polarizer axis perpendicular to the plane of incidence. The sample is connected to a sample holder on the refrigerator head using copper-loaded vacuum grease and it can be be cooled to temperatures as low as 24 K. Visible light from a stabilized source is directed to the refrigerator head by a thick-core (400 μm) fused-silica fibre, and is collimated into a parallel beam, before passing through

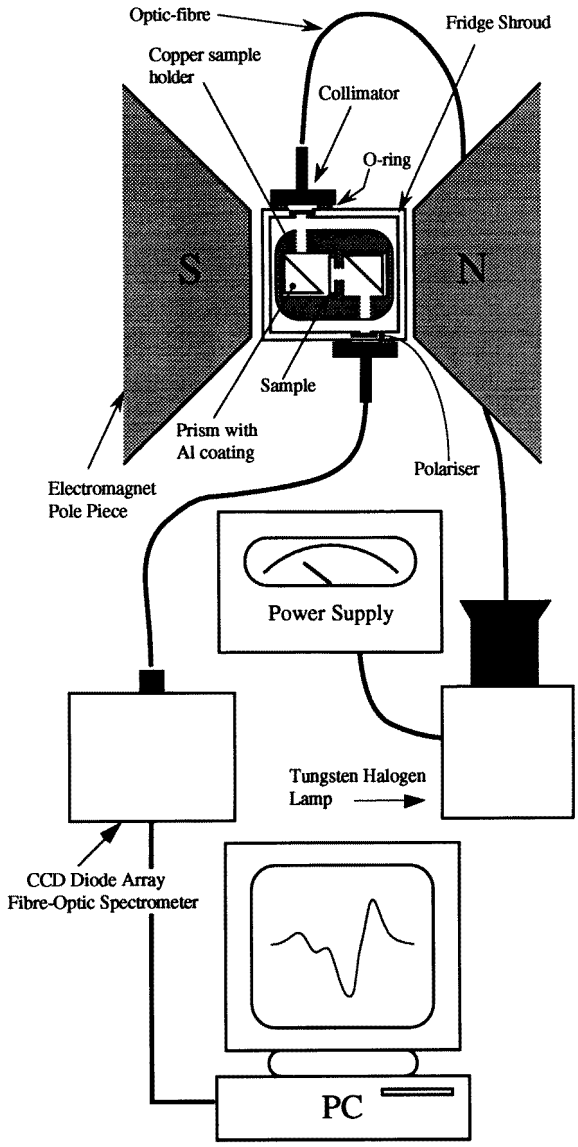

Figure 2. The apparatus used for wavelength- and temperature-dependent Faraday rotation measurements.

the sample in the Faraday geometry. The output fibre has a 100 μm fused-silica core and is matched to the spectrometer, so that a 500 nm spectral range can be registered over a 1024-pixel array at 0.5 nm per pixel.

To measure the Faraday rotation, a transmission spectrum of the sample is taken both with the magnetic field on and with it turned off. Then it can be shown that the dispersive Faraday rotation $\theta_F(\lambda)$ is given by

$$\theta_F(\lambda) = \frac{1}{2}\left[\sin^{-1}\left(\frac{I_B(\lambda)}{I_0(\lambda)} - 1\right)\right] \tag{1}$$

where $I_B(\lambda)$ and $I_0(\lambda)$ are the wavelength-dependent transmitted intensities with the magnetic field on and off respectively. In equation (1), the small effect due to Faraday ellipticity has been neglected, which is a good approximation in the spectral region of interest where $n \gg k$. The apparatus described above was also used to record absorption and transmission spectra in the absence of the magnetic field.

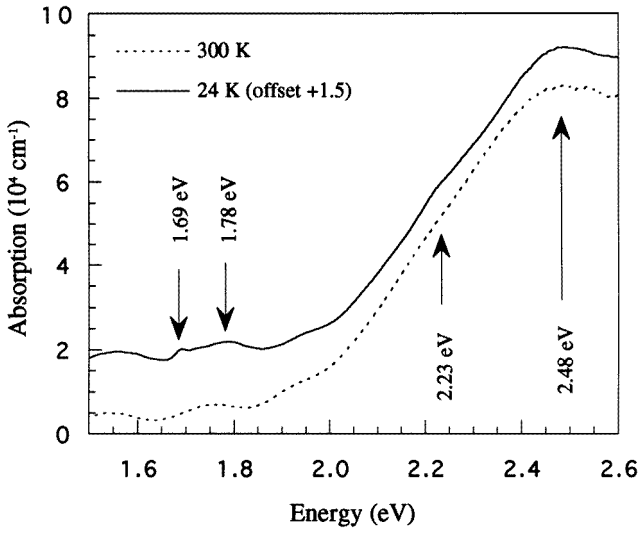

Figure 3. The temperature-dependent optical absorption of a $BaFe_{12}O_{19}$ film, in the 1.5 eV–2.6 eV energy range. The 24 K spectrum is offset by 1.5×10^4 cm^{-1}. Comparison of the two spectra at low energies reveals absorption features superimposed on Fabry–Perot oscillations.

3. Results and discussion

Figures 3 and 4 show the temperature-dependent absorption and Faraday rotation spectra of a $BaFe_{12}O_{19}$ film 1 μm thick. Immediately noticeable is the appearance of detailed structure at low temperatures, particularly in the Faraday rotation spectrum, where at 24 K a number of distinctive transitions can be resolved. An expanded view of this structure in the range 1.6–1.9 eV is presented in figure 5, showing the location of two different types of transition with paramagnetic and diamagnetic lineshapes. The strongest of these transitions occurs at 1.69 eV with a positive paramagnetic lineshape, according to the sign convention of Scott *et al* [12]. We suggest that this is the $^6A_{1g}(^6S) \rightarrow {}^4T_{2g}(^4G)$ crystal-field transition originating on octahedrally coordinated Fe^{3+} sites. The spectral range of investigation is not wide enough to include the higher-energy transitions from these sites, thus precluding fitting to a Tanabe–Sugano diagram for which a number of transitions are required. However, the assignment is probable, in view of the facts that a band of equivalent transitions in octahedrally coordinated Fe^{3+} in yttrium iron garnet (YIG), occurs at nearly the same energy (1.68–1.85 eV) [12], and that crystal-field transitions in sites with cubic symmetry are generally observed to have paramagnetic magnetooptic lineshapes.

It is possible to estimate the oscillator strength f of the 1.69 eV transition using a

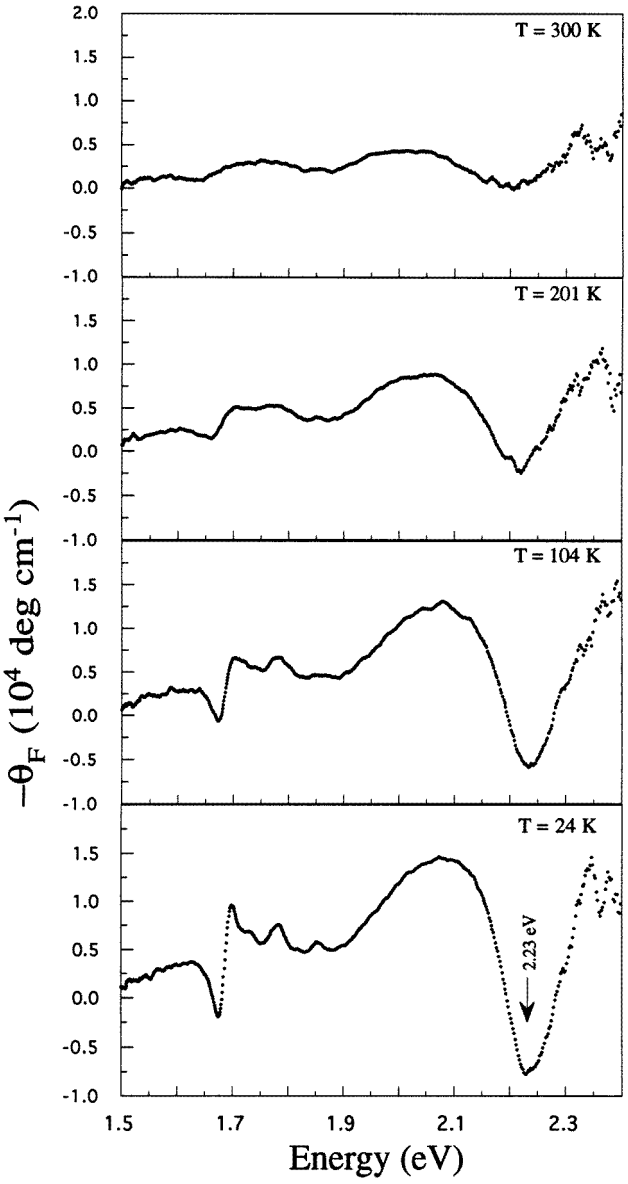

Figure 4. The temperature-dependent Faraday rotation of a $BaFe_{12}O_{19}$ film, between 1.5 eV and 2.4 eV.

version of the formula given by Suits [13], in SI units, namely

$$f = \frac{4cmn\varepsilon_0\Gamma}{Ne^2}\theta_{\mathrm{Fp}} \tag{2}$$

where c is the speed of light in vacuum, e and m are the electron charge and rest mass respectively, n is the refractive index, ε_0 is the vacuum permittivity, Γ is the linewidth measured as the peak-to-peak energy separation, N is the number of $4f_2$ cations per unit volume, and θ_{Fp} is the peak-to-peak height of the lineshape. In the case of $BaFe_{12}O_{19}$,

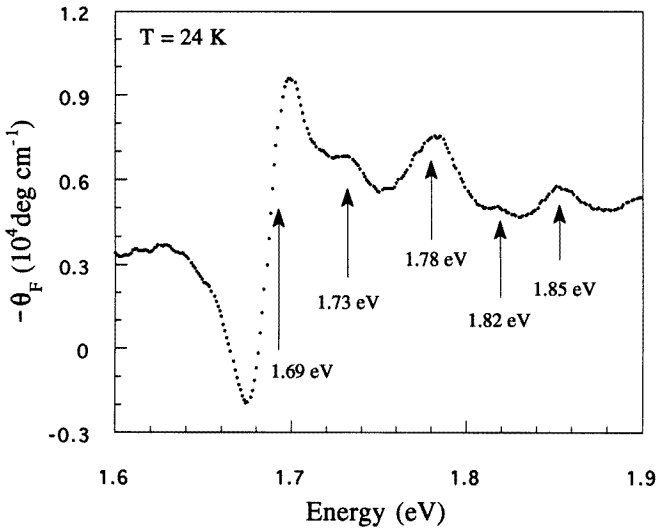

Figure 5. An expanded view of the detailed structure in the 24 K Faraday rotation spectrum of figure 3. Positions of various transitions are indicated.

there are four $4f_2$ cations per unit cell of volume 2.1×10^{-27} m^3. Using this, and measured values for θ_{Fp} and Γ of 1.14×10^4 deg cm^{-1} and 26 meV respectively, and a refractive index of $n = 3$ from reference [14], the oscillator strength from the 24 K spectrum of figure 4, was calculated to be 5×10^{-2}. This value is very large as compared to that for the main $^6A_{1g}(^6S) \rightarrow {}^4T_{2g}(^4G)$ transition in YIG, which was found by Scott *et al* to have an oscillator strength of 2×10^{-5} [15].

It is suggested that, due to its observed strength, the 1.69 eV transition originates specifically on the $4f_2$ octahedral site (there being three octahedral sites in the $BaFe_{12}O_{19}$ crystal structure). This is justified by the fact that, as the $4f_2$ site shares a face with the neighbouring Ba^{2+} ion, some admixture of the large Ba^{2+} 5p orbital moment with the Fe^{3+} ion across the shared face might be expected, which would make the d–d transition less strongly forbidden. Furthermore, the ions on $4f_2$ sites are exchange coupled to the Fe^{3+} ions on 2b trigonal bipyramidal sites with an exchange constant which is the strongest in the structure [8]. This may also contribute to the strength of the transition, as exchange coupling between magnetic ions relaxes the spin and parity selection rules [16, 17]. Finally, weaker paramagnetic transitions originating on the 12k and 2a octahedral sites might, according to the above scheme, be eclipsed by the $4f_2$ transition, if they were lying at the same energy.

The other transitions observed in the fine structure of figure 5 occur with positive diamagnetic lineshapes between 1.73 eV and 1.85 eV. We suggest that these may originate on the 2b trigonal bipyramidal site because of the observed lineshape difference, although an understanding of the mechanism responsible for lineshape variations in crystal-field transitions is needed to substantiate this. Nevertheless, the approximate energy of the diamagnetic lineshapes corresponds reasonably well with the expected location of the first-excited-state transition from the $^6A_1(^6S)$ ground state, according to the energy level diagram calculated by Fuchikami [18], and using the suggested values for the crystal-field splitting parameters of $d_2 = 8300$ cm^{-1}, and $d_4 = 1800$ cm^{-1} (similar to $10Dq$ in the cubic case). The existence of more than one diamagnetic transition in figure 5 might be due to some symmetry-breaking mechanism such as the dynamic Jahn–Teller effect, where the bipyramid

distorts during the lifetime of the transition to remove the excited-state degeneracy, in addition to the presence of magnon or phonon sidebands.

Table 1. Suggested transition assignments of the various spectral features as discussed in the text. Where appropriate, the same transition in YIG is listed for comparison (after reference [12]). The subscript on $^4E_{(1)}$ refers to the first excited state.

Assignments of transitions from the ground state	Type ($BaFe_{12}O_{19}$)	Energy (eV) ($BaFe_{12}O_{19}$)	Energy (eV) (YIG)
$^4T_{2g}(^4G)$ ($4f_2$ site)	+ve paramagnetic	1.69	1.81
$^4E_{(1)}$ (2b trigonal bipyramidal site)	+ve diamagnetic	1.73–1.85	
$^4T_2(^4G)$	+ve paramagnetic or −ve diamagnetic	2.30 or 2.23	2.37
$^4E, {}^4A_1(^4G)$		2.48	2.57

Finally, we suggest that the broad feature in figure 4, above 2.10 eV (at 24 K), is due to a transition in the $4f_1$ tetrahedral site. Specifically, the extrema at 2.23 eV and 2.35 eV might be associated with a positive paramagnetic lineshape centred at 2.30 eV, and resulting from the $^6A_1(^6S) \rightarrow {}^4T_2(^4G)$ transition. The same transition in YIG, also paramagnetic, is centred at 2.37 eV [12]. On the other hand, the 2.23 eV peak occurs at about the same energy as a feature in the 24 K absorption spectrum of figure 3, suggesting that the transition is centred at this energy rather than at 2.30 eV. This being the case, the lineshape would have to be interpreted as being diamagnetic, which is unusual given the observation of a paramagnetic lineshape in YIG, and that paramagnetic lineshapes are associated with crystal-field transitions in sites with cubic symmetry. Table 1 lists the various transitions under discussion along with the suggested assignments.

It is clear from the present work that further investigation is needed to fully justify the proposed transition assignments. This will require the recording of low-temperature optical and magnetooptical spectra up to significantly higher energies than are currently achieved, to include higher-lying transitions from the various Fe^{3+} sites and thus perform fits to the respective energy diagrams, in addition to examining the various lineshapes and oscillator strengths. In addition, molecular orbital cluster calculations for the trigonal bipyramidal site, which have not, to our knowledge, been performed, would be necessary to determine the onset of metal-to-ligand charge-transfer transitions, as these would be expected to occur at higher energies of several eV, around the energies of higher-lying crystal-field transitions.

4. Conclusions

In conclusion, we have examined for the first time to our knowledge, the low-temperature Faraday rotation spectrum of $BaFe_{12}O_{19}$, and have observed fine structure at 24 K between 1.69 eV and 1.85 eV in the form of a strong paramagnetic lineshape and a number of weaker diamagnetic lineshapes. It is proposed that the paramagnetic and diamagnetic transitions are associated with crystal-field transitions on Fe^{3+} sites with octahedral and trigonal bipyramidal coordination respectively, and a broader higher-energy feature at 2.30 eV results from transitions in tetrahedrally coordinated Fe^{3+} sites. The assignments made have been based on the position of equivalent transitions in the more well characterized YIG, and on

the observation of the transitional lineshapes. Finally, additional work has been proposed to clarify the present results, based on the investigation of optical and magnetooptical spectra up to higher energies to include additional crystal-field transitions.

Acknowledgment

The authors would like to acknowledge some very helpful discussions with Z Simsa during the preparation of this work.

References

[1] Kojima H 1982 *Ferromagnetic Materials* ed E P Wolfharth (Amsterdam: North-Holland) ch 5
[2] Morisako A, Matsumoto M and Naoe M 1988 *IEEE Trans. Magn.* **24** 3024
[3] Morisako A, Matsumoto M and Naoe M 1987 *IEEE Trans. Magn.* **23** 56
[4] Naoe M, Hasunuma S, Hoshi Y and Yamanaka S 1981 *IEEE Trans. Magn.* **17** 3184
[5] Shono K, Gomi M and Abe M 1982 *Japan. J. Appl. Phys.* **21** 1451
[6] Nakamura H, Ohmi F, Kaneko Y, Sawada Y, Watada A and Machida H 1989 *J. Appl. Phys.* **61** 3346
[7] Simsa Z, Stichauer L, Kolacek J, Pointon A J and Turner C 1991 *J. Magn. Magn. Mater.* **101** 233
[8] Smit J and Wijn H P J 1965 *Ferrites* (Eindhoven: Philips Technical Library) ch 3
[9] Zanmarchi G and Bongers P F 1969 *J. Appl. Phys.* **40** 1230
[10] Drews U and Jaumann J 1969 *Z. Angew. Phys.* **26** 48
[11] Masterson H J, Lunney J G, Coey J M D, Atkinson R, Salter I W and Papakonstantinou P 1993 *J. Appl. Phys.* **73** 3917
[12] Scott G B, Lacklinson D E, Ralph H I and Page J L 1975 *Phys. Rev.* B **12** 2562
[13] Suits J C 1972 *IEEE Trans. Magn.* **8** 95
[14] Papakonstantinou P 1994 *PhD Thesis* Queen's University of Belfast
[15] Scott G B, Lacklinson D E and Page J L 1974 *Phys. Rev.* B **10** 971
[16] Lohr LL 1972 *Coord. Chem. Rev.* **8** 241
[17] Sherman D M 1985 *Am. Mineral.* **70** 1262
[18] Fuchikami N J 1965 *J. Phys. Soc. Japan* **20** 760